Beauty with environmental symbiosis — development of a topical cosmetic solution with moisture permeability control technology that responds to external humidity conditions

Sogabe, Atsushi*; Ohtani, Tsuyoshi; Gillet, Renaud; Lin, Kuanting; Masuda, Kazuki; Kondo, Mika; Hirose, Kenta; Murata, Daichi; Knight, Christopher Takaya; Miyai, Masashi

MIRAI Technology Institute, Shiseido Co., Ltd., Yokohama, Japan

* Corresponding author: Atsushi Sogabe, 1-2-11, Takashima, Nishi-ku, Yokohama 220-0011, JAPAN
+81-45-22-1600; atsushi.sogabe@shiseido.com

Abstract

Global warming and climate change have increased awareness of how humans interact with the environment. In particular, human skin is exposed to environmental changes that affect it in various ways. Therefore, in the present study we developed technologies to mitigate external environmental changes, focusing on humidity.

The response of the occlusion effect to humidity was evaluated by determining the dependence of water vapor permeability on humidity. The humidity responsiveness mechanism was inferred from the water content, and from the results of differential scanning calorimetry, Fourier-transform infrared spectroscopy, X-ray diffraction, and molecular dynamics (MD) simulations. Human tests and 3D skin model tests were conducted to verify the efficacy of the humidity-responsive material with respect to the skin.

We found that, among general cosmetic ingredients, polyvinyl alcohol (PVA) had the desired humidity response, i.e., high water vapor permeability at high humidity and low water vapor permeability at low humidity. We confirmed that the water content of PVA gradually changed in response to humidity, and its crystallinity changed accordingly, which affected its vapor permeability. MD simulations demonstrated the same tendency for the changing diffusion coefficient of water.

PVA also exhibits changes in vapor permeability on human skin. It increased the moisture content of the stratum corneum more at lower humidity levels than at higher humidity levels. Moreover, humidity-responsive materials may inhibit damage caused by

dryness compared with materials that do not respond to humidity. We will apply this technology to the preparation of cutting-edge beauty products that adapt to the environment.

1. Introduction

In recent years, the world has faced unprecedented environmental changes, including global warming, localized heavy rain, and extremes of temperature. Among the many environmental factors that affect the skin [1], humidity is of great interest to consumers. Products are being developed in response to regional characteristics and seasonal changes in relation to humidity. With great improvements in indoor humidity control technologies, skin is increasingly exposed to rapid changes in humidity between outdoor and indoor environments. The effects of low humidity on the skin have been widely studied [2-5]. Recently, there has been research on the effects of high humidity caused by wearing medical masks during the COIVD-19 pandemic [6]. It is desirable to address both low and high humidity changes.
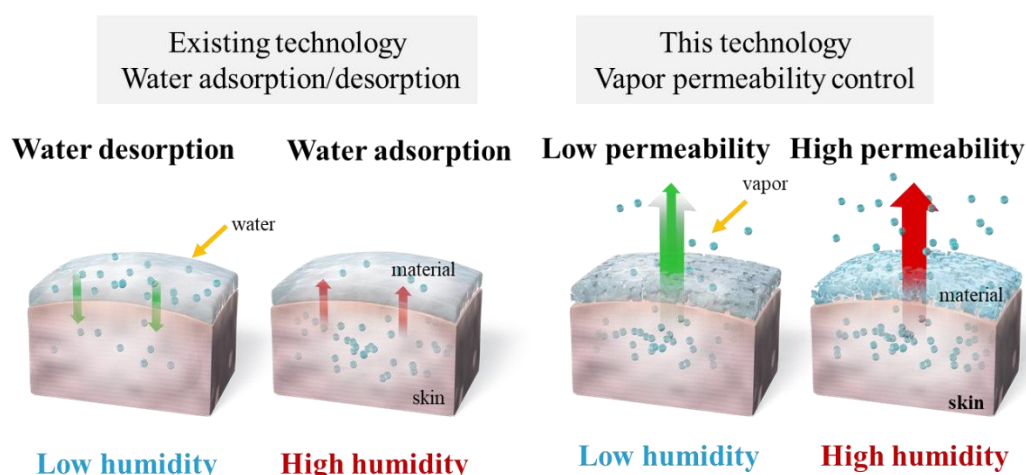

Figure 1. Concept of humidity responsive technology

Our goal is to develop a technology that mitigates sudden humidity changes, prevents skin damage, and allows customers to live more actively without worrying about environmental changes. As a method of mitigating humidity differences, we were inspired by traditional Japanese houses. Japanese houses are made of wood and are designed to be comfortable during the four seasons without using electricity. General moisture control

technologies for houses can be classified into water vapor absorption/desorption and vapor permeability control. Vapor absorption/desorption is applied in cosmetics [7,8], but its effect is limited by the amount of water that can be absorbed or desorbed. Herein, we aim to apply vapor permeability control technology, a new technology that has not yet been realized as a function of cosmetics, to create fast-responding cosmetics that provide lasting effects and protect the skin. Using the technology developed in the present study, we aim to form a barrier that can withstand humidity differences and protect the skin from the resulting negative influences. This could take the form of a cream, emulsion, makeup, or some similar solution.

2. Materials and methods

2.1 Materials

Filter paper (filter paper 5A; Kiriyama Glass Works Co.), polyvinyl alcohol (PVA; GOHSENOL EG-05C; Mitsubishi Chemical Co.), glycerin (Sakamoto Yakuhin Kogyo Co., Ltd.), Vaseline (Vaseline P; VNS-P; Nikko Rika Co.), liquid paraffin (High White 22S; MORESCO Corporation), squalane (NIKKOL Purified Olive Squalane; Nikko Chemicals Co., Ltd.), and silicone elastomer (dimethicone/vinyl dimethicone cross polymer; KSG-16; Shin-Etsu Chemical Co., Ltd.) were used as received.

2.2 Sample preparation

PVA films were prepared by pouring a PVA solution of a predetermined concentration (0.5–10 wt%) onto a polystyrene dish, and maintaining it at room temperature for at least two nights. The other sample membranes were prepared by applying 50 mg of the raw material to a filter paper (3.5 cm^2). Complex membranes of PVA and raw material were prepared by overlaying the sample membranes described above on a PVA membrane. The weight ratio of PVA to the raw material was 1:3 (w/w).

2.3 Evaluation of humidity responsiveness of the occlusive effect and vapor permeability

There are several methods for measuring water vapor permeability. They can be classified into the differential pressure method [9] and the isobaric pressure method [10]. Herein, the wet cup method [11], which is an isobaric pressure method, was selected and arranged for material evaluation. It was chosen because it is simple, it enables the evaluation of a large number of samples, and it realistically simulates vapor evaporation from the skin.

A certain amount of water was placed in a glass sample tube and the top of the tube was covered with the prepared membrane. The side of the membrane to which the sample had been applied was exposed to air. The composite membrane was set so that the PVA membrane overlapped the air side of the sample membrane (Figure 2). The sample tube was placed in a humidity-controlled chamber at a predetermined temperature. The rate of water volatilization was measured under various humidity conditions using an electronic scale.
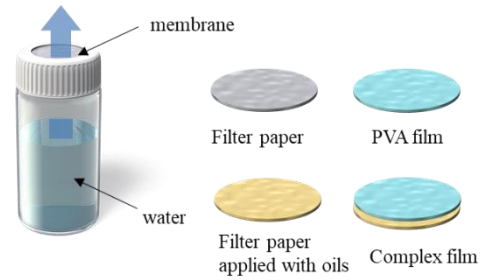

Figure 2. Schematic illustration of method for evaluating humidity responsiveness

The water vapor permeability at each humidity level was calculated using vapor pressure differences to evaluate the humidity dependence of the moisture permeability:

$$rate\ of\ water\ loss = \frac{w_1[g] - w_0[g]}{surface\ area[m^2] \times time[h]} \tag{1}$$

$$vapor\ permeability = \frac{rate\ of\ water\ loss\ [g/m^2h]}{P_{inside}[Pa] - P_{outside}[Pa]} \tag{2}$$

where w_0 and w_1 are the weight of the samples before and after measurement, $P_{outside}$ is the external humidity (which we set), and P_{inside} is the humidity inside the vial (herein assumed to be 100% relative humidity).

2.4 Evaluation of moisture content of PVA

The PVA films were cut into discs, each with a radius of 2.5 mm. Each film was placed in a decompression dryer for 24 h, then weighed. Next, each film was placed in a humidity chamber set to the specified humidity conditions, and weighed again after 24 h. The water content was calculated using the following equation:

$$water\ content[\%] = \frac{w[g] - w_d[g]}{w[g]} \times 100 \tag{3}$$

where w and w_d are the weights of the samples subjected to the specific humidity and drying conditions.

2.5 Differential scanning calorimetry (DSC)

The PVA film was sealed in an aluminum pan, and the enthalpy of melting water (ΔH) was measured using a differential scanning calorimeter (SSC/5200; Seiko Instruments Inc.). The temperature scanning conditions were as follows. First, the equilibrium state was checked at 30°C. The sample was then cooled to -40°C at a rate of 2°C/min, and the equilibrium state was maintained at that temperature for 5 min. The temperature was then

increased to 30°C at a rate of 1°C/min, and ΔH was measured. The free water content was determined from the value of ΔH taking the heat required to melt 1g of water as 334 J, and the total water content minus the free water content was used to determine the amount of bound water.

2.6 X-ray diffraction (XRD)

The crystallinity of the PVA film was evaluated using an X-ray diffractometer (RINT-TTR III; Rigaku Corporation). The concentration method was used because the surfaces of the samples were smooth. The measurement range was 3 to 60°, and a non-reflective plate was used as the substrate. The samples were stored under various humidity conditions to evaluate the humidity response, and the XRD patterns were obtained immediately after. The humidity was adjusted using the following saturated aqueous solutions: LiCl 11%RH, $MgCl_2$ 33%RH, $Mg(NO_3)_2$ 54%RH, NaCl 75%RH, and K_2SO_4 97%RH.

2.7 Fourier-transform infrared spectroscopy (FT-IR)

The PVA films were stored under the various humidity conditions described in Section 2.6., and were evaluated using a Fourier-transform infrared spectrometer (NICOLET 6700; Thermo Fisher). The attenuated total reflection method was used for the measurements.

2.8 Molecular dynamics (MD) simulation

All-atom molecular dynamics calculations were performed using J-OCTA system (JSOL Corporation). A 20-mer of PVA (of which 2 monomers are acetylated) was prepared and the position of the acetylated monomers was determined randomly. A generalized AMBER force field was applied, and restrained electrostatic potential charges based on electrostatic potentials calculated using B3LYP/6-31G(d) density functional theory were used for the point charges. One hundred polymer molecules were randomly placed in the simulation cell (initial density 0.3 g/cm^3). After polymer placement, the desired number of water molecules was added at random positions.

First, NVT-MD was executed for 5 ps at 300 K to obtain a condensed structure. Second, the structure was pre-equilibrated by NTP-MD for 2 ns in the cubic cell under 100 MPa at 300 K. This was followed by equilibration for an additional 100 ns (time step dt = 1 fs for all calculations). We used Gromacs-2019.4 software. The charge calculation was conducted using the Particle Mesh Ewald algorithm.

The solubility coefficient S (cm^3 (STP)/cm^3 Pa) and the diffusion coefficient D (cm^2/s)

were then analyzed, and the permeability coefficient P (cm^3 (STP) cm/cm^2 s Pa) was calculated from the equation P = S×D.

2.9 Human test

A panel of 15 volunteers of either gender (20–49 years old) was recruited for the human test. We used a total of four sites (two on each arm); each site comprised a 9 cm^2 area on the inner side of the upper arm. Samples were applied at four levels: unapplied, 0.76 mg/cm^2 PVA, 3.0 mg/cm^2 PVA, and 3.0 mg/cm^2 silicone elastomer. Trans-epidermal water loss (TEWL) (Tewameter® TM 300; Courage+Khazaka electronic GmbH) and moisture content (Corneometer® CM 825; Courage+Khazaka electronic GmbH) were measured at 26%RH and 67%RH in 23°C before and 30 min after sample application, and the difference was evaluated. These protocols for human tests were approved by the ethics committee of Shiseido Research Ethics Committee (Yokohama, Japan). Statistical analysis was performed using a Bonferroni–Dunn multiple comparisons test.

2.10 3D skin model test

2.10.1 Cell culture – humidity responsiveness test

An EpiDerm™ FT-400 kit was stored on a six-well culture plate and equilibrated in EFT medium for 24 h at 37°C (5% CO_2). Prior to recurrent exposure to low humidity, a 7.0 cm × 9.5 cm window was cut from the lid of the six-well plate, and the opening was sealed with filter paper, filter paper with silicone elastomer, or filter paper with PVA. 3D skin models were then cultured at 95% humidity for 12 h and at 20% humidity for 12 h. Culture was continued for a further 48 h. The tissue was then removed from its cassette and the epidermis layer was isolated for further mRNA analysis.

2.10.2 mRNA isolation and quantitative reverse transcription polymerase chain reaction (qRT-PCR) analysis

The epidermis layer of EpiDerm™ FT-400 was homogenized using zirconia/silica beads. RNA was isolated using Isogen (NIPPON GENE CO., LTD.). mRNA was converted to cDNA using a GoScript™ Reverse Transcription System (Promega), and the cDNA was used as a template for evaluating expression using a LightCycler® 480 SYBR® Green I Master kit (Roche) on a LightCycler® 480 II system (Roche).

2.11 Statistical analysis

The data pertaining to the properties of the materials are expressed as means ± SDs, and those from the human test and 3D skin model test are expressed as means ± SEs. The

statistical analysis of the human test data was performed using a Bonferroni–Dunn multiple comparisons test, and the statistical analysis of the qRT-PCR data was performed using one-way analysis of variance followed by a Tukey's multiple comparisons test.

3. Results

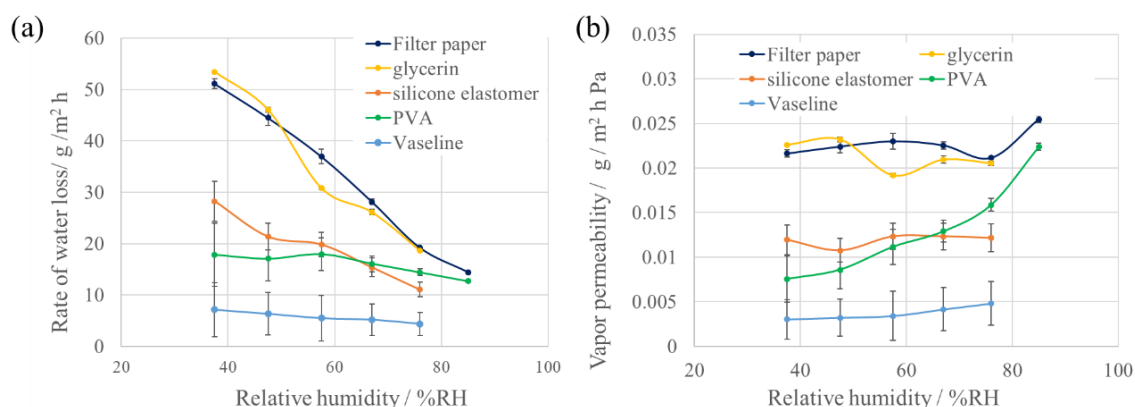### 3.1 Humidity responsiveness of the raw materials

Figure 3. Humidity responsiveness of raw materials. (a) Rate of water loss, (b) vapor permeability. Data represent the mean ± SD, n=3–4.

The rate of water loss from bare filter paper, filter paper coated with certain cosmetic ingredients and PVA film at various humidity levels and 28°C are shown in Figure 3 (a). The rate of water loss from the filter paper not coated with cosmetic ingredients changed proportionally to the change in humidity. Glycerin is known to increase the water content of the stratum corneum, but has no occlusion effect on its own, whereas PVA, silicone elastomer, and Vaseline have occlusion effects. Vapor permeability, which was calculated from the rate of water loss and the difference in vapor pressure, is shown in Figure 3 (b). The vapor permeability of silicone elastomer and Vaseline remained almost constant with changing humidity. The vapor permeability of the PVA was approximately the same as that of filter paper at 85%RH. However, the vapor permeability at 37%RH was 1/3 that at 85%RH.

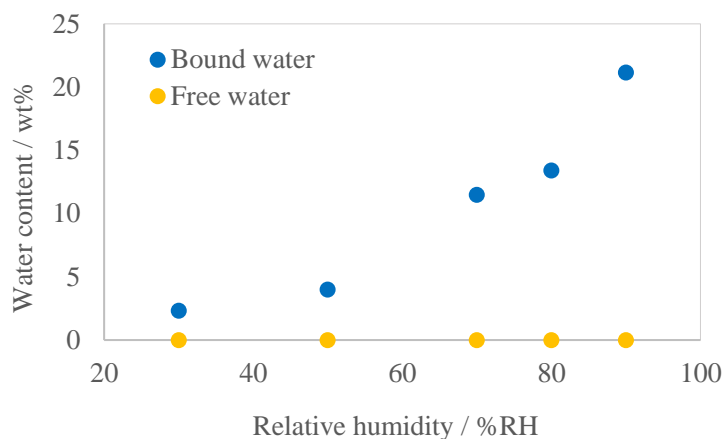## 3.2 Mechanism of humidity responsiveness of PVA

Figure 4. Content and properties of water in the polyvinyl alcohol films. Data represent the averages of two experiments.

The water content of PVA at various humidity levels was measured using the gravimetric method, and the properties of the water in the PVA were also investigated by DSC. The water content in PVA varied with humidity, and the maximum water content was approximately 20% (Figure 4). The DSC results showed that most of the water in the PVA was bound water, and no free water was detected.
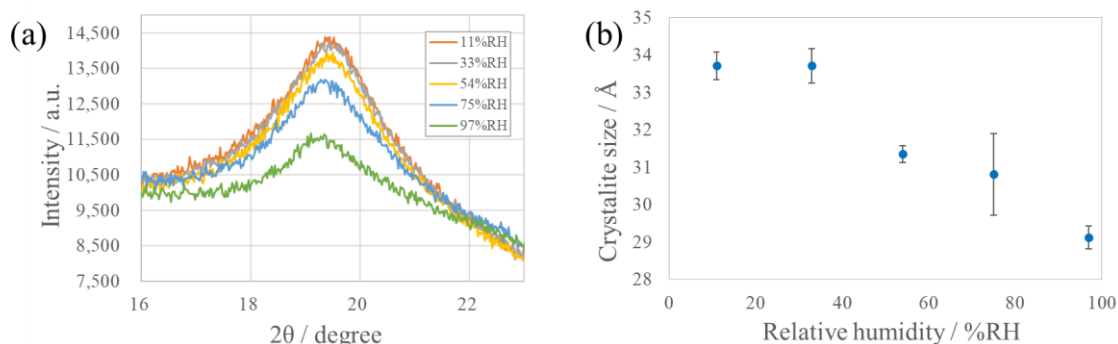

Figure 5. X-ray Diffraction (XRD); (a) XRD spectrum, (b) crystallite size. XRD measurements were performed immediately after the PVA films were taken from the desiccators. Data represent the mean ± SD, n=3.

XRD patterns were obtained at various humidity levels, and the XRD peaks broadened as the humidity increased (Figure 5 (a)). Crystallite size was used as an index of crystallinity, and the value decreased as the humidity increased (Figure 5 (b)).
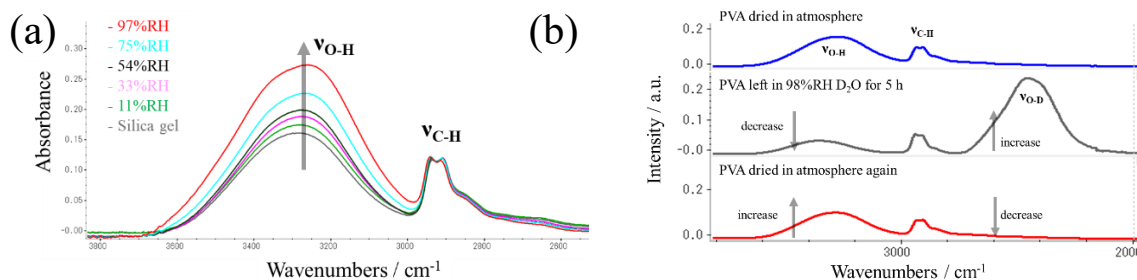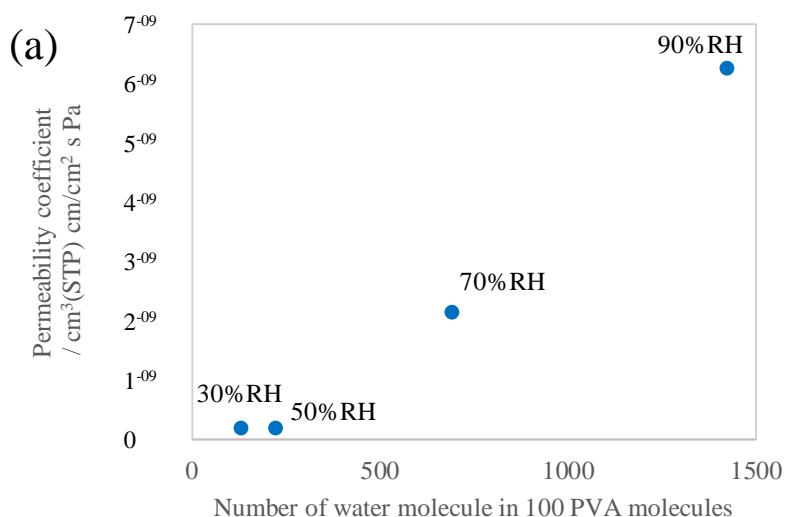
Figure 6. Fourier-transform infrared spectrometry (FT-IR); (a) FT-IR spectra at various humidity levels with H_2O; FT-IR measurements were obtained immediately after the PVA films were taken from the desiccators. (b) FT-IR spectra demonstrating the replacement of H_2O by D_2O.

IR measurements at various humidity levels revealed a change in the H_2O-derived peak at approximately 3250 cm^{-1}, indicating that the amount of water in the PVA film changed in response to changes in external humidity (Figure 6 (a)). When PVA was dissolved in deuterated water (D_2O) and dried to form a membrane, the membrane contained H_2O under dry conditions, but was free of D_2O. PVA membranes left in 90%RH D_2O for 5 h demonstrated that the H_2O in the membrane had been replaced with D_2O (Figure 6 (b)). When the PVA film was subsequently left in an atmospheric environment again, the D_2O in the membrane was replaced by H_2O.
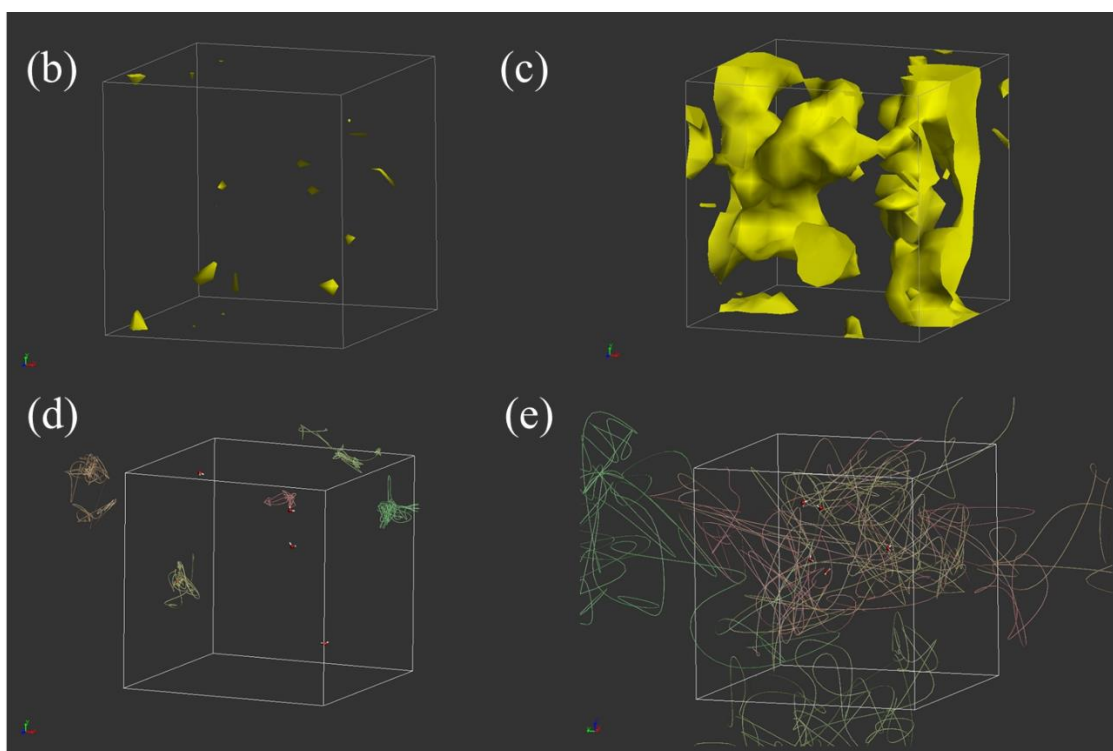
Figure 7. Diffusion coefficient of water molecules determined by molecular dynamics (MD) simulation; (a) humidity dependence of diffusion coefficient; (b) density distribution of water at 30%RH; (c) at 90%RH; (d) Snapshot of traces of five water molecules at 30%RH; (e) at 90%RH. Five water molecules in the PVA film were scrutinized and their 100 ns trajectories were drawn.

Figure 7 (a) shows the water permeability coefficient for water molecules placed in the calculated cell according to the water content at each humidity level. It was confirmed that as the number of water molecules increased, the permeability coefficient, which is the product of the solubility coefficient and the diffusion coefficient, increased. The density distribution of water in the PVA film following the addition of water molecules corresponding to low and high humidity is shown in Figure 7 (b) and (c). The water molecules exist in scattered locations at low humidity, whereas at high humidity they exist in a continuous location. A snapshot of the 100 ns trajectory of five molecules of water is also shown in Figure 7 (d) and (e). At low humidity, the diffusion distance of the water is short, but at high humidity it is long.
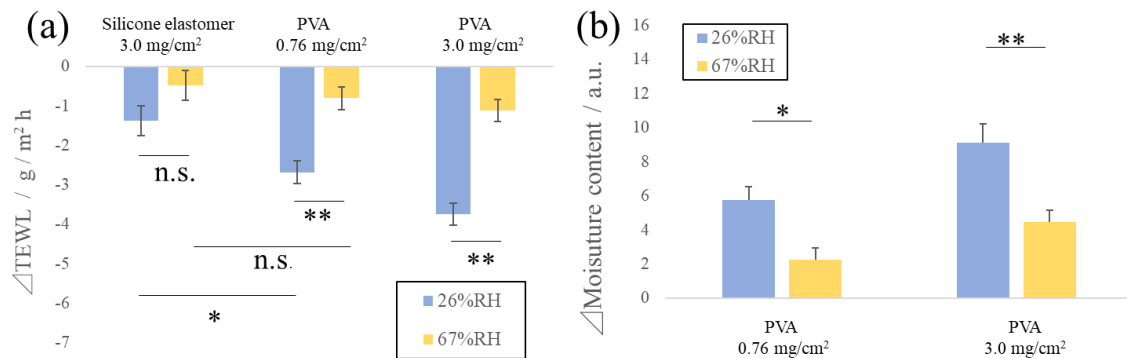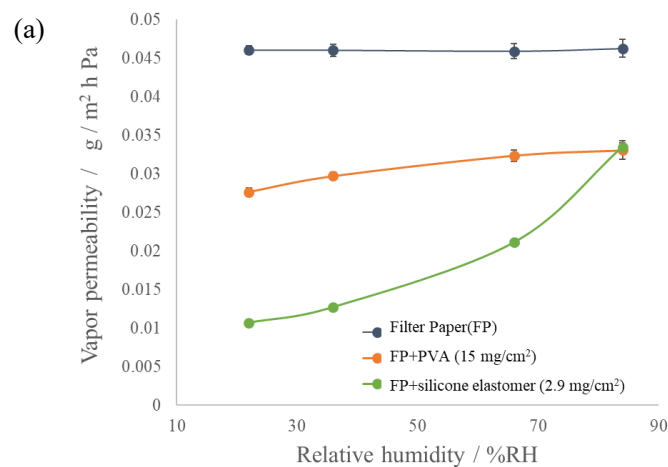
3.3 Effects of humidity-responsive materials

Figure 8. Human test. (a) Trans-epidermal water loss (TEWL); (b) moisture content. Data represent the mean ± SE, n=15. p-values were calculated using the Bonferroni–Dunn multiple comparisons test (*: $p < 0.05$, **: $p < 0.01$)

The effect of humidity responsiveness on human skin was verified by the human test. The changes in TEWL and moisture content before and after the application of the sample are shown in Figure 8 (a) and (b), where the changes in the unapplied area are subtracted. The silicone elastomer reduced TEWL and demonstrated an occlusion effect, but there was no significant difference at various humidity levels. However, PVA demonstrated the same level of occlusion as that of the silicone elastomer at high humidity, and the occlusion effect increased significantly at low humidity. The degree of occlusion varied depending on the thickness of the applied film, and the effect was observed even when the amount was reduced to 1/4 that of the silicone elastomer. The measurement of skin moisture content immediately after PVA peeling showed that skin moisture increased more at low humidity than at high humidity.
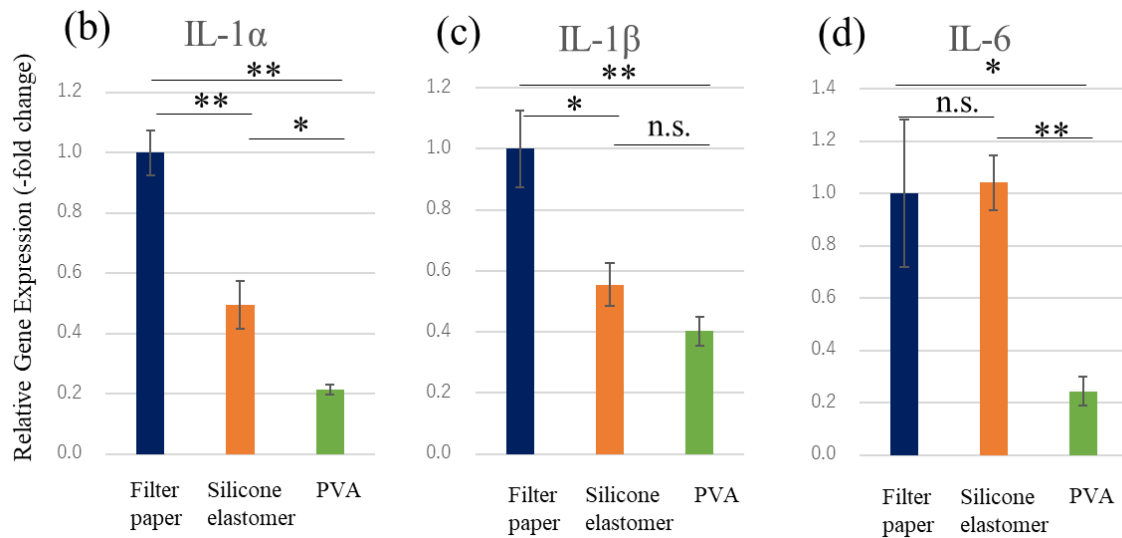
Figure 9. Humidity responsiveness of the samples in the 3D skin model test; (a) vapor permeability at 37°C. Data represent the mean ± SD, n=3-4; relative gene expression (b) IL-1α, (c) IL-1β, (d) IL-6. Data represent the mean ± SE, n=4–6. p-values were calculated using the Tukey's multiple comparisons test (*: $p < 0.05$, **: $p < 0.01$)

The vapor permeability values of the membranes used in the 3D skin model test at 37°C are shown in Figure 9 (a). Compared with filter paper, the silicone elastomer had lower permeability, but exhibited almost no humidity response. The PVA had the same degree of permeability as the silicone elastomer at high humidity, but at low humidity, the degree of permeability decreased to approximately 40% of that at high humidity.

The results of the gene expression analysis of IL-1α and a series of other interleukins as an index of dryness stress [12] are shown in Figure 9 (b) - (d). The expression of IL-1α was significantly lower with the silicone elastomer compared with the filter paper, and was even more significantly suppressed with PVA compared with the silicone elastomer. The analysis of other factors including IL-1β and IL-6 exhibited the same trend of decreased expression with PVA, although it was not significant for all of them.
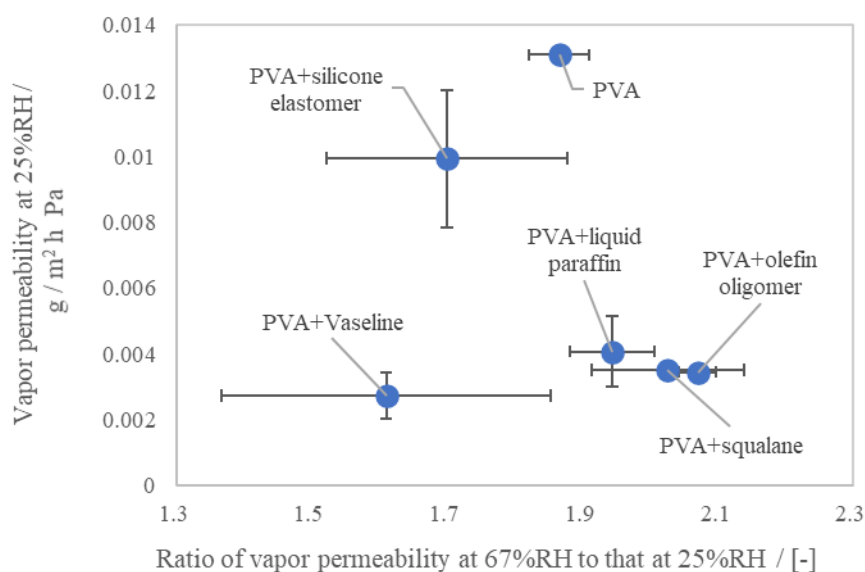
3.4 Cosmetic applications

Figure 10. Relative change in vapor permeability of a complex film. The x-axis shows the ratio of vapor permeability at 67%RH to that at 25%RH as an index of humidity responsiveness; the y-axis shows the vapor permeability at 25%RH. Data represent the mean ± SD, n=4–5.

The water vapor permeability at 25%RH was measured for PVA and a bilayer film consisting of PVA and filter paper with oil. The vapor permeability was reduced to approximately 1/3 of the maximum. Comparing the permeability at 67%RH and 25%RH as an index of humidity response, the humidity response was not impaired in any of the oil combinations. In terms of combinations with oils, the humidity response tended to improve in combinations comprising the olefin oligomer, squalane, and liquid paraffin.

4. Discussion

4.1 Humidity responsiveness of the raw materials

Materials with water vapor permeability values that change in response to humidity were first investigated, focusing on food packaging films. With regard to food packaging, a constant vapor permeability is desired to maintain the freshness of the food under various environmental conditions [13,14]. Among such film materials, PVA and ethylene vinyl alcohol copolymers (PE-PVA) have low water vapor permeability values at low humidity, but their performances decrease at high humidity [14-20]. Therefore, the challenge is to improve permeability at high humidity, and various modifications have been attempted [20]. We considered that PVA and PE-PVA have the desired properties. Furthermore, as

mentioned in the Introduction Section, the construction industry is also developing technologies to mitigate external environmental changes. Polyethylene (PE) film is used to release humidity from a room during humid summer weather, and to maintain humidity during humid winter weather [21]. Among the candidate materials, PE-PVA is insoluble in cosmetic solvents, which makes its formulation difficult. In contrast, PVA has long been utilized as a water-soluble filming agent for cosmetics, and has been used to impart a feeling of firmness to the skin. In the present study, we focused on this material with the aim to utilize it as a humidity-responsive material. First, we decided to verify the humidity responsiveness of PVA under actual environmental conditions.

Using PVA films prepared in a laboratory environment, we confirmed that water vapor permeability can change in response to humidity (Figure 3). This is a unique property that is not seen in the moisturizers and oils used as common cosmetic ingredients. Furthermore, although the results are not included in the text, the vapor permeability response to humidity is reversible from low to high humidity or from high to low humidity.

4.2 Mechanism of humidity responsiveness of PVA

The humidity dependence of the rate of water loss of PVA is a known phenomenon and is believed to be due to the change in the hydrogen bonding of its hydroxyl groups [14,15]. We used several techniques to better understand the mechanism underlying the water vapor permeability of PVA.

In the present study, the water content of the PVA changed in response to humidity; most of the water molecules were bound water, and interacted with the PVA (Figure 4). The XRD patterns revealed a stepwise change in crystallite size, indicating that the water incorporated into the PVA film affected its crystal structure (Figure 5). The IR measurements obtained in a D_2O atmosphere revealed that the water in the PVA film could be reversibly replaced (Figure 6), confirming that the bound water in the PVA film had sufficient mobility to exchange with the water molecules in the atmosphere. MD simulation of the water vapor permeability of the amorphous part of the PVA membrane showed that the diffusion coefficient changed with the water content (Figure 7). This suggests that the mechanism of the change in water vapor permeability is due to the stepwise changes in water content and crystallinity in response to changes in humidity, which affect the structure of the PVA film.

4.3 Effects of humidity-responsive materials

A human test and a 3D skin model test were performed to evaluate the usefulness of the humidity responsiveness of PVA. The vapor permeability, in other words the occlusion

effect, of PVA applied to human skin changes in response to external humidity (Figure 8). In addition, we confirmed that under low humidity conditions, during which the skin tends to dry out easily [3-5], the vapor permeability decreases, thereby increasing the moisture content improvement effect compared with materials that are unresponsive to humidity. PVA is therefore expected to have superior ability in terms of maintaining the moisture content of the skin at a constant level in response to changes in external humidity. A 3D skin model test was conducted to confirm this humidity-responsive effect at the cellular level. The indices of dryness damage were reduced using PVA compared with the other materials that were unresponsive to humidity (Figure 9). It is assumed that the reduction in vapor permeability at low humidity by PVA resulted in a constant rate of water loss, which suppressed the damage caused by dryness.

4.4 Cosmetic applications

PVA has long been used as a firming agent for cosmetics or facial mask products, but to the best of our knowledge, there have been no attempts to use it as a vapor permeability control material. In the present study, we investigated various combinations of PVA and oils to prepare a humidity-responsive base material, and discovered an appropriate combination that improves the occlusive effect without compromising the humidity-responsive property. In addition, although the problem of aggregation is often experienced when large amounts of PVA are used, we discovered that the amount of PVA can be reduced by combining it with appropriate oils, which improve the feel of the product. We plan to develop new formulations based on these findings.

5. Conclusions

To create a technology that mitigates sudden humidity changes, we searched for an appropriate material with a permeability that changes with humidity, and found that PVA and its derivatives have suitable properties. The mechanism by which PVA responds to humidity was inferred to be a change in its structure due to the change in water content, which affects the diffusivity of water in the PVA film.

The human test revealed that the rate of water loss from the skin changed in response to external humidity, and that PVA was highly effective at increasing the moisture content of the skin at low humidity. The 3D skin model experiments also suggested that humidity-responsive materials effectively reduce the damage caused by drying. To apply the PVA to cosmetic formulations, we investigated the effects of using it in combination with common oils, and discovered a combination that enhances the humidity responsiveness of some oils.

We aim to apply this technology to the preparation of cutting-edge cosmetics that will protect the consumer by minimizing the occlusive effect at higher humidity levels, but also provide protection in dry conditions. This technology will respond to changes in humidity, protecting the skin before those changes can have a negative impact, and helping consumers live in comfort, undaunted by changes in their environment.

6. Acknowledgments

We would like to thank Mr. Keita Nishida and Ms. Saki Kamada (Brand Value R&D Institute, Shiseido Co., Ltd.) for their useful contributions to discussions about the application of the composition.

7. Conflict of interest statement

NONE

8. References

1. Engebretsen KA, Johansen JD, Kezic S, et al (2016) The effect of environmental humidity and temperature on skin barrier function and dermatitis. J Eur Acad Dermatol Venereol 30:223–249
2. Grice K, Sattar H, Sharratt M, et al (1971) The effect of ambient humidity on transepidermal water loss. J Invest Dermatol 57:108–110
3. Egawa M, Oguri M, Kuwahara T, et al (2002) Effect of exposure of human skin to a dry environment. Skin Research and Technology 8:212–218
4. Sunwoo Y, Chou C, Takeshita J, et al (2006) Physiological and subjective responses to low relative humidity. Journal of Physiological Anthropology 25:7–14
5. Tsukahara K, Hotta M, Fujimura T, et al (2007) Effect of room humidity on the formation of fine wrinkles in the facial skin of Japanese. Skin Research and Technology 13:184–188
6. Hua W, Zuo Y, Wan R, et al (2020) Short-term skin reactions following use of N95 respirators and medical masks. Contact Dermatitis 83:115–121
7. Flavikafine, Nisshinbo Chemical Inc.
8. Sato T, Teramatsu Y, Nakane T (1996), SEN'I GAKKAISHI 52:20-26
9. ISO (International Organization for Standardization) 15105-1 (2007) Plastics -Film and sheeting- Determination of gas-transmission rate - Part 1: Differential-pressure methods. Available at https://www.iso.org/standard/41677.html (accessed 06/18/2022).

10. ISO (International Organization for Standardization) 15105-2 (2003) Plastics -Film and sheeting- Determination of gas-transmission rate - Part 2: Equal-pressure method. Available at https://www.iso.org/standard/37514.html (accessed 06/18/2022).

11. ASTM (ASTM International) E96-95 (1995) Standard Test Methods for Water Vapor Transmission of Materials. Available at https://www.astm.org/e0096-95.html (accessed 06/18/2022).

12. Ashida Y, Ogo M, Denda M (2001) Epidermal interleukin-1α generation is amplified at low humidity: implications for the pathogenesis of inflammatory dermatoses. Br J Dermatol 144:238–243

13. Marsh K, Bugusu B (2007) Food packaging--roles, materials, and environmental issues. J Food Sci 72:R39–R55

14. Katsura T. (2008) Gas-barrier polymers for packaging materials. Kobunshi 57:974–977

15. Yu X, Wang A, Cao S (1987) Water-vapor permeability of polyvinyl alcohol films. Desalination 62:293–29

16. Tsujita Y. (2010) Fundamentals of permeability and barrier properties of gases and water vapor through polymeric membrane and films. Journal of The Surface Finishing Society of Japan 61:675–681.

17. Chen M, Wang Y, Wang L, et al (2014) Effects of temperature and humidity on the barrier properties of biaxially-oriented polypropylene and polyvinyl alcohol films. Journal of Applied Packaging Research 6:40–46

18. Zhang Z, Britt IJ, Tung MA. (2001) Permeation of oxygen and water vapor through EVOH films as influenced by relative humidity. Journal of Applied Polymer Science 82:1866–1872

19. Muramatsu M, Okura M, Kuboyama K, et al (2003) Oxygen permeability and free volume hole size in ethylene–vinyl alcohol copolymer film: temperature and humidity dependence. Radiation Physics and Chemistry 68:561–564

20. Maes C, Luyten W, Herremans G, et al (2018) Recent updates on the barrier properties of ethylene vinyl alcohol copolymer (EVOH): a review. Polymer Reviews 58:209–246

21. Tyvek® smart, DuPont-Asahi Flash Spun Products Co., Ltd.